Pharmaceutical Research, Vol. 24, No. 8, August 2007 (© 2007)
DOI: 10.1007/s11095-006-9231-y

Research Paper

Dendritic α,ε-Poly(L-lysine)s as Delivery Agents for Antisense Oligonucleotides

Khee Dong Eom,[2] Sun Mi Park,[1] Huu Dung Tran,[1] Myong Soo Kim,[1] Ri Na Yu,[3] and Hoon Yoo[1,4]

Received June 21, 2006; accepted December 26, 2006; published online March 21, 2007

Purpose. To evaluate the potential use of dendritic α,ε-poly(L-lysine)s (DPL) for the efficient cellular delivery of antisense oligonucleotides.
Methods. A series of dendritic α,ε-polylysines of various generations were prepared. Their physical properties and the ability to form complex with oligonucleotide were investigated by polyacrylamide gel electrophoresis, capillary zone electrophoresis (CZE), agarose gel electrophoresis, fluorescence titration and atomic force microscopy (AFM). The efficiency to deliver oligonucleotide to HeLa cells, stably transfected with plasmid pLuc/705, was evaluated by using antisense splicing correction assay and confocal microscopy.
Results. DPLs formed the complexes with antisense oligonucleotide with modest cytotoxicity. The charge ratio of oligonucleotide to DPL and the size (generation) of DPLs were all critical variables for the antisense effect. Compared to low generation DPLs, high generation DPLs were more effective in delivering oligonucleotide into cells.
Conclusions. High generation DPL-oligonucleotide complexes were moderately effective for delivery antisense oligonucleotide. The complex formation provides a promise for *in vivo* therapeutic application of DPLs or their derivatives in the delivery of gene or oligonucleotide.

KEY WORDS: antisense oligonucleotide; delivery; dendritic α,ε-poly(L-lysine).

INTRODUCTION

The cationic polymers draw substantial interest in the field of gene/oligonucleotide including siRNA delivery due to their advantages such as simplicity, non-immunogenicity, and low toxicity in clinical application (1–3). Several synthetic polycations such as liposome, polyethylenimine (PEI), poly(L-lysine) (PLL) and cationic PAMAM dendrimers have been widely used to transfer gene or oligonucleotide into cells (4–12). However, the poor transfection efficiency of cationic polymers, compared to viral vectors, limits the clinical application of these agents (13–15).

Recently we reported the facile synthesis and physical properties of the novel dendritic polymers consisting of dendritic α,ε-poly(L-lysine)s (16). The prepared DPLs are similar to PAMAM dendrimers with well-defined structure and precise number of surface amines, but consist of amino acids, L-lysine residues, as a branch unit. DPLs are cationic spherical polymers with positively charged primary lysine amino groups on surface at physiological condition. DPLs form stable complexes with plasmid DNAs with limited cell toxicity, and with considerable effectiveness in gene transfer at the cell culture level (8,16).

Little is known about the mechanism of DPL mediated cellular uptake of gene or oligonucleotide. It has been suggested internalization through endocytosis may be the main pathway for cationic polymer/DNA complexes. The transfection properties of cationic polymers such as PAMAM dendrimers were influenced significantly by the size, surface charge, heterodispersity and molecular weight of the generation, indicating that the structural features and surface properties of DPLs may also play important roles for the effective transfection of gene/oligonucleotide (14–18).

In this study, to investigate the characteristics of DPLs in the delivery of oligonucleotide, various DPL generations were prepared by using the solid-phase peptide synthesis method and investigated for their physical properties, interaction with oligonucleotide and delivery efficiency of oligonucleotide into cell. The physical properties of DPLs

[1] Department of Pharmacology and Dental Therapeutics, College of Dentistry, Chosun University, 375 Seosuk-dong, Dong-gu, Gwangju 501-759, South Korea.
[2] Nanormics Inc., Sungbuk-gu, Seoul 136-130, South Korea.
[3] Department of Food Science and Nutrition, University of Ulsan, Mugeo-dong, Nam-ku, Ulsan 680-749, South Korea.
[4] To whom correspondence should be addressed. (e-mail: hoon_yoo@chosun.ac.kr

ABBREVIATIONS: AFM, atomic force microscopy; Boc, tertiary-butoxycarbonyl; CZE, capillary zone electrophoresis; DCHA, dicyclohexylammonium; DIEA, N,N-diisopropylethylamine; DMF, dimethylformamide; DPL, dendritic α,ε-poly(L-lysine); Fmoc, fluorenylmethoxycarbonyl; HOBt, N-hydroxybenzotriazole; MALDI TOF-MS, matrix assisted laser desorption ionization time-of-flight mass spectrometry; MBHA, 4-methylbenzhydrylamine; MTT, 3-(4,5-dimethyl-2-thiazoyl)-2,5-diphenyl-2H-tetrazolium bromide; PAGE, polyacrylamide gel electrophoresis; PAMAM, polyamidoamine; PEI, polyethylenimine; PLL, poly(L-lysine); TFA, trifluoroacetic acid; 2-Cl-Z, 2-chlorobenzyloxycarbonyl.

were investigated in terms of molecular size and shape by comparing elution times in electrophoretic mobilities of capillary zone electrophoresis and mobilities in a non-denatured polyacrylamide gel electrophoresis. The DPLs formed stable complexes with oligonucleotide, and the complex formation was size and shape dependant with modest cytotoxicity. The charge ratio of oligonucleotide to DPL, and the size (generation) of DPLs were all critical variables for the antisense effect. High generation DPLs, generation 5 and generation 6, were more effective in delivering oligonucleotide into cells than low generation DPLs.

MATERIALS AND METHODS

Materials

PAMAM dendrimer was a generous gift from Dr. R. L. Juliano (University of North Carolina at Chaple Hill). SYBR

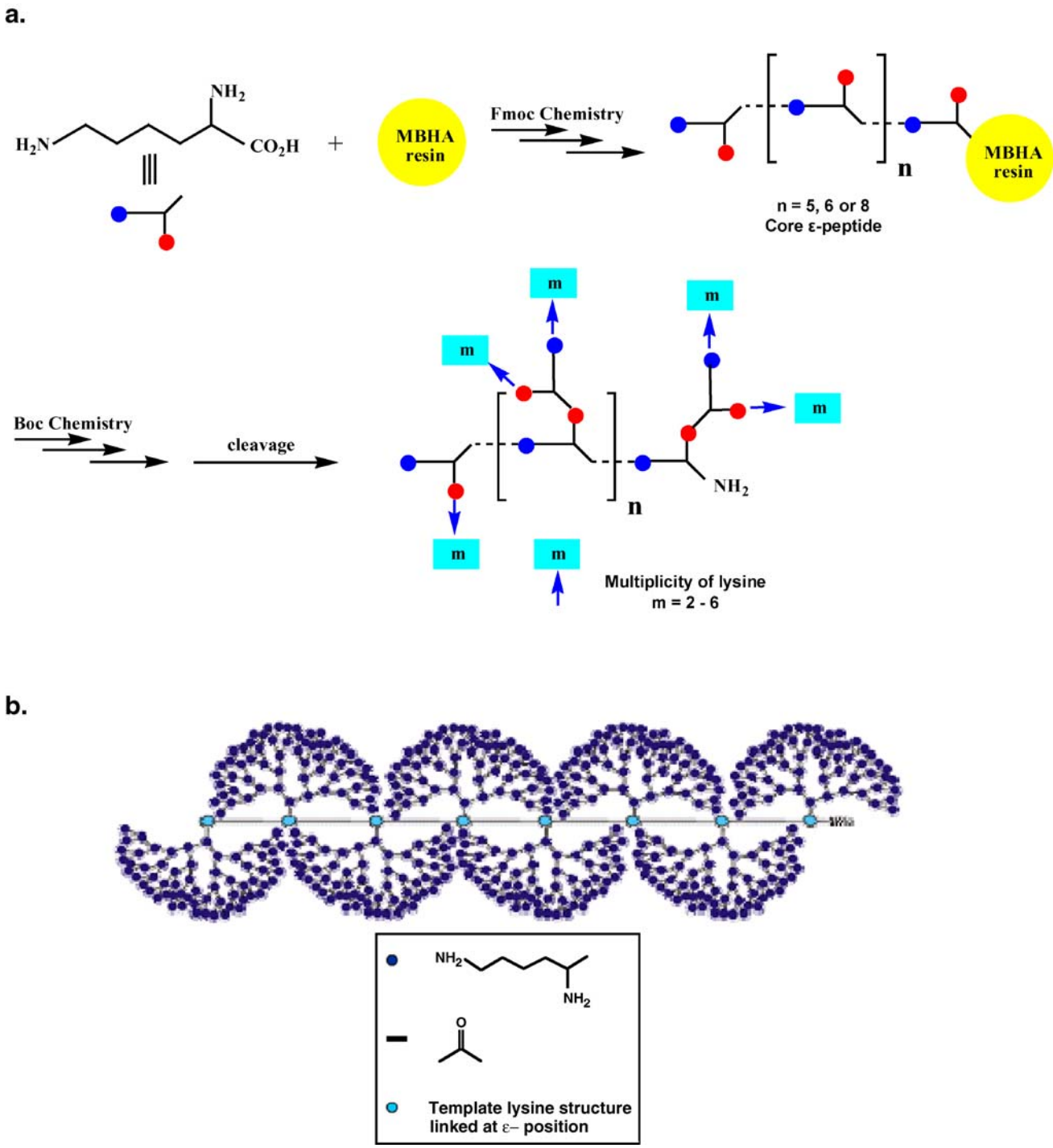

Fig. 1. Schematic structure and synthetic route of various generation of dendritic α,ε-poly(L-lysine)s (DPLs); **a**: (a) Fmoc chemistry; Boc-L-Lys(Fmoc)-OH, DCC, HOBt·1/2H_2O, 20% piperidine, (b) Boc chemistry; Boc-L-Lys(Boc)-OH·DCHA, DCC, HOBt·1/2H_2O, 50% TFA, (c) Cleavage; TFMSA/thioanisole/TFA(1:1:10, v/v/v), 4–6 h. **b**: The representative structure of DPL generation 6 (NC-12).

Table I. The Number of Surface Amino Groups and the Molecular Weight of DPLs

DPL	Generation	Number of Surface Amino Groups	Number of Lysine Residues in Core ε-peptide	Observed Mass (m/z)
NC-4	2	32	8	4,118.8
NC-6	3	48	6	6,170.1
NC-7	4	80	5	10,272
NC-8	5	180	5	20,526
NC-9	3	64	8	8,223.7
NC-10	4	128	8	16,668
NC-11	5	256	8	33,303
NC-12	6	512	8	65,328[a]

[a] The observed mass peak of NC-12 was very weak and broad.

Green I and Oregon green 488 were purchased from Molecular Probes (Eugene, OR, USA) and prepared in DMSO (1 mg/ml). DMEM and Opti-MEM were from Life Technologies (Gaithersburg, MD). Lipofectin was obtained from Gibco BRL (Baltimore, MD). A phosphorothioate 2′-O-methyl oligonucleotide (5′-CCUCUUACCUCA GUUACA-3′) and corresponding 3′-TAMRA-labeled derivative were purchased from the Midland Certified Reagent Company (Midland, TX). HeLa cells stably transfected with plasmid pLUC/705 were a generous gift of Dr R. Kole (University of North Carolina, Chapel Hill, NC). All other chemicals including poly L-lysine hydrobromide (MW 55700) were from Sigma Chemical (St. Louis, MO, USA).

Preparation of Dendritic α,ε-Poly(L-lysine)s

Synthetic procedures that were used to prepare dendritic α,ε-poly(L-lysine)s were described in previous report (16,19). Briefly, DPLs were synthesized by preparing the epsilon-peptide template (a peptide consisting of five, six or eight lysine residues) as an initiator core. A DPL of the first generation was synthesized by coupling Boc-L-Lys(Boc)-OH·DCHA on a low substituted MBHA resin by the DCC/HOBt coupling method. DPLs of the second to sixth

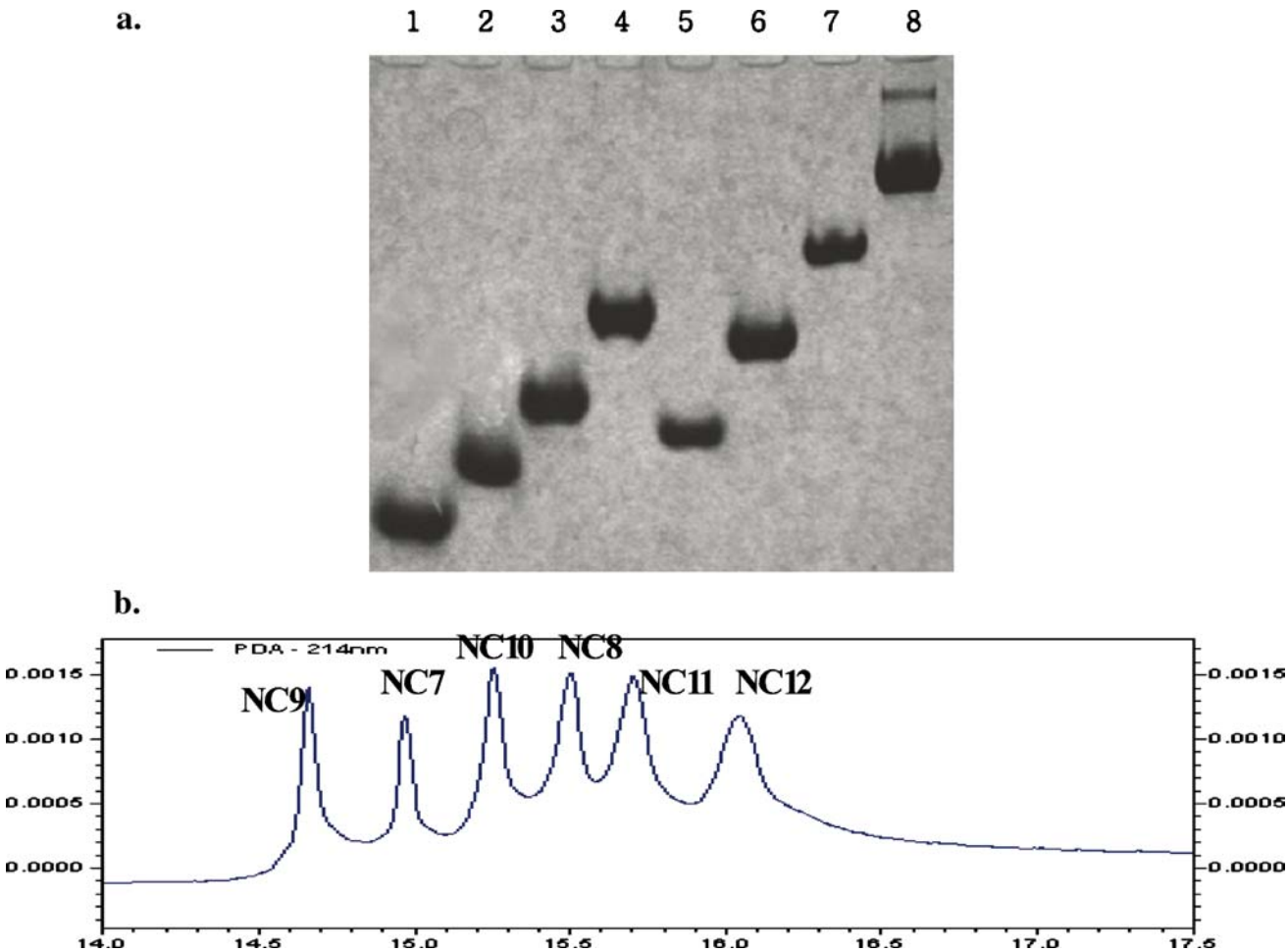

Fig. 2. Electrophoretic mobility of DPLs. DPLs were separated by polyacrylamide gel electrophoresis and capillary zone electrophoresis. (**a**) 10% PAGE experiment: samples were loaded onto gels in a buffer composed of 15% glycerol, 0.025% bromophenol blue and 0.1 mM EDTA and electrophoresed for 90 min at 100 V: lane1; NC-4 (30 μg), lane 2; NC-6 (20 μg), lane 3; NC-7 (20 μg), lane 4; NC-8 (20 μg), lane 5; NC-9 (20 μg), lane 6; NC-10 (30 μg), lane 7; NC-11 (20 μg), lane 8; NC-12 (30 μg). (**b**) CZE: the capillary was conditioned as described in "MATERIALS AND METHODS" Individual peak identification of six DPLs (NC-7, NC-8, NC-9, NC-10, NC-11, NC-12) was done prior to the injection of the mixture.

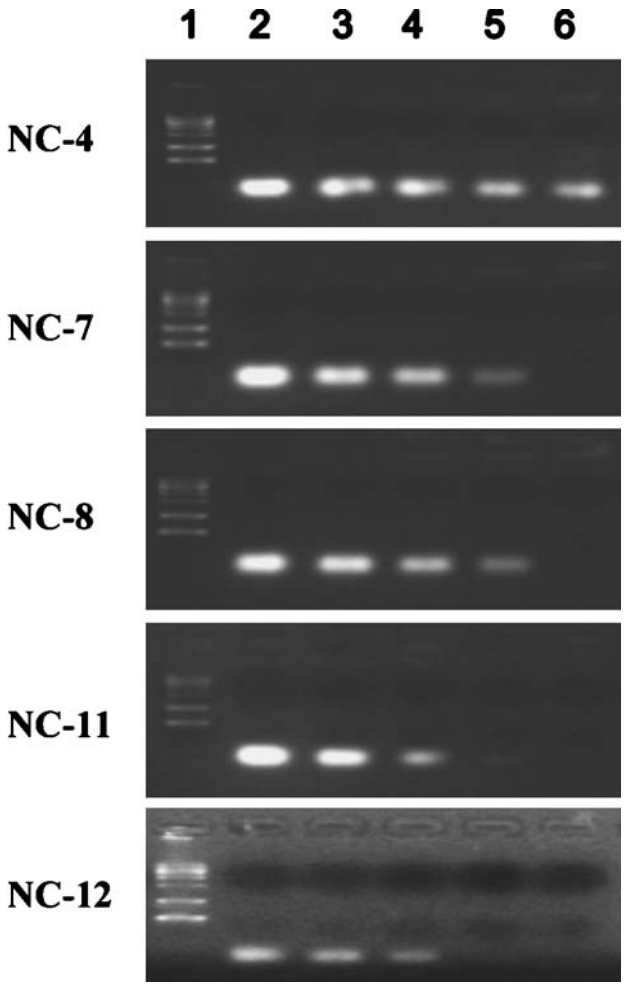

Fig. 3. Agarose gel electrophoresis of phosphorothioate oligonucleotide/DPL complexes. The complexes were prepared as described in experimental details. Various concentrations of oligonucleotide were added to the 1 μg of DPL in TBE buffer. The N/P charge ratios (amino groups : phosphate groups) are as follows: lane 1, 100 bp DNA ladder; lane 2, oligonucleotide only (60 μM); lane 3, N/P charge ratio 2.5; lane 4, 7.5; lane 5, 12.5; lane 6, 25.

generations were obtained by coupling Boc-L-Lys(Boc)-OH·DCHA repeatedly after deprotection with TFA (Fig. 1). A Kaiser test, which detects residual free amino groups, was performed at each coupling step. HPLC for purification was performed in a Waters Delta Prep 4000 system with Vydac C18 column (4.6 × 250 mm, 5 μm).

Molecular Weight Determination by MALDI-TOF

Mass spectra were obtained on matrix-assisted time-of-flight mass spectrometry (MALDI TOF-MS) using PerSeptive Biosystem Voyager-DE STR instrument (USA). α-Cyano-4-hydroxy-cinnamic acid was used as a matrix for NC-4 to NC-9, and 3,5-dimethoxy-4-hydroxy-cinnamic acid was used for NC-10, -11, and -12.

Analytical Conditions of the CZE Separation

CZE was carried out with a constant voltage at 20°C using a P/ACE MDQ Capillary Electrophoresis System (BECKMAN COULTER) equipped with a standard cassette containing an uncoated fused-silica capillary (50 μm I.D. × 72.5 cm long: effective length = 60.0 cm) and a photodiode array detector. The capillary was conditioned before injection by washing with 0.1 M sodium hydroxide, then ultra pure water, and finally with the running buffer (200 mM phosphate : acetonitrile, 2:1 volume ratio, pH 1.5). The sample solutions (1 mg/ml in running buffer) were loaded onto the capillary with a pressure mode. Electrophoresis was run with a voltage of 15 kV and an average current of 65 μA. Electrophoretograms were recorded at 214 nm by monitoring the wavelength (16,20).

Atomic Force Microscopy

A 100 μl of α,ε-polylysines/oligonucleotide complexes in water (0.1 μg/ml) were deposited onto the center of a freshly split untreated silicone wafer. The wafer surface was dried at room temperature before taking the image using an AFM. A Nanoscope version 4.31 controller with a multimode AFM (Digital Instrument, Santa Barbara, CA) and Si_3N_4 cantilevers (MicroMasch company) with spring constants of 20-75 Nm^{-1} were used for imaging. AFM images were collected in a tapping mode at room temperature. High-resolution topographic image of sample surface was obtained by using a scanning technique for conductors and insulators on an atomic scale at the scanning rate of 1.10 Hz.

Fluorescent Dye Exclusion Assay

Binding properties of DPLs with oligonucleotide were examined by a fluorescent titration assay using fluorescence microplate reader (TECAN). Oligonucleotide was mixed with DPLs, polylysine or PAMAM dendrimer generation 5 (MW 28826), in various N/P ratios. After standing for 5 min at room temperature, 100 μl of SYBR Green I solution (1:10,000 dilution in 10 mM TE buffer) was added to the DPL-oligonucleotide mixtures. The fluorescence was measured by exciting at 485 nm while monitoring emission at 535 nm.

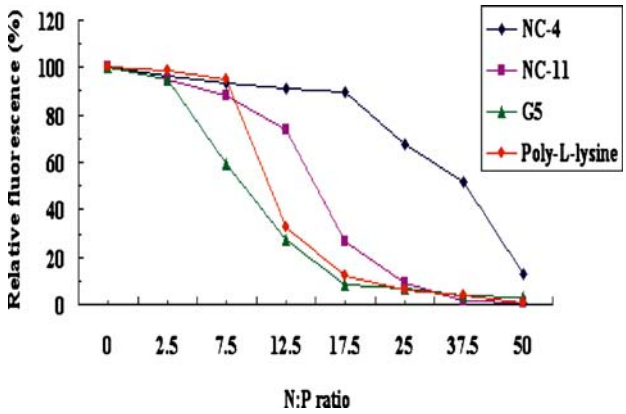

Fig. 4. Fluorescence titration assay. Oligonucleotide (50 μM) was mixed with NC-4, NC-11, PAMAM G5, and poly(L-lysine) at various N/P ratios. After standing for 5 min at room temperature, 100 μl of SYBR Green I solution (1:10,000 dilution in 10 mM TE buffer) was added to the complex solution. The fluorescence of the dye was measured on a fluorescence microplate reader by exciting at 485 nm while monitoring emission at 535 nm. G5 indicates PAMAM dendrimer generation 5. Data represent the average of three experiments.

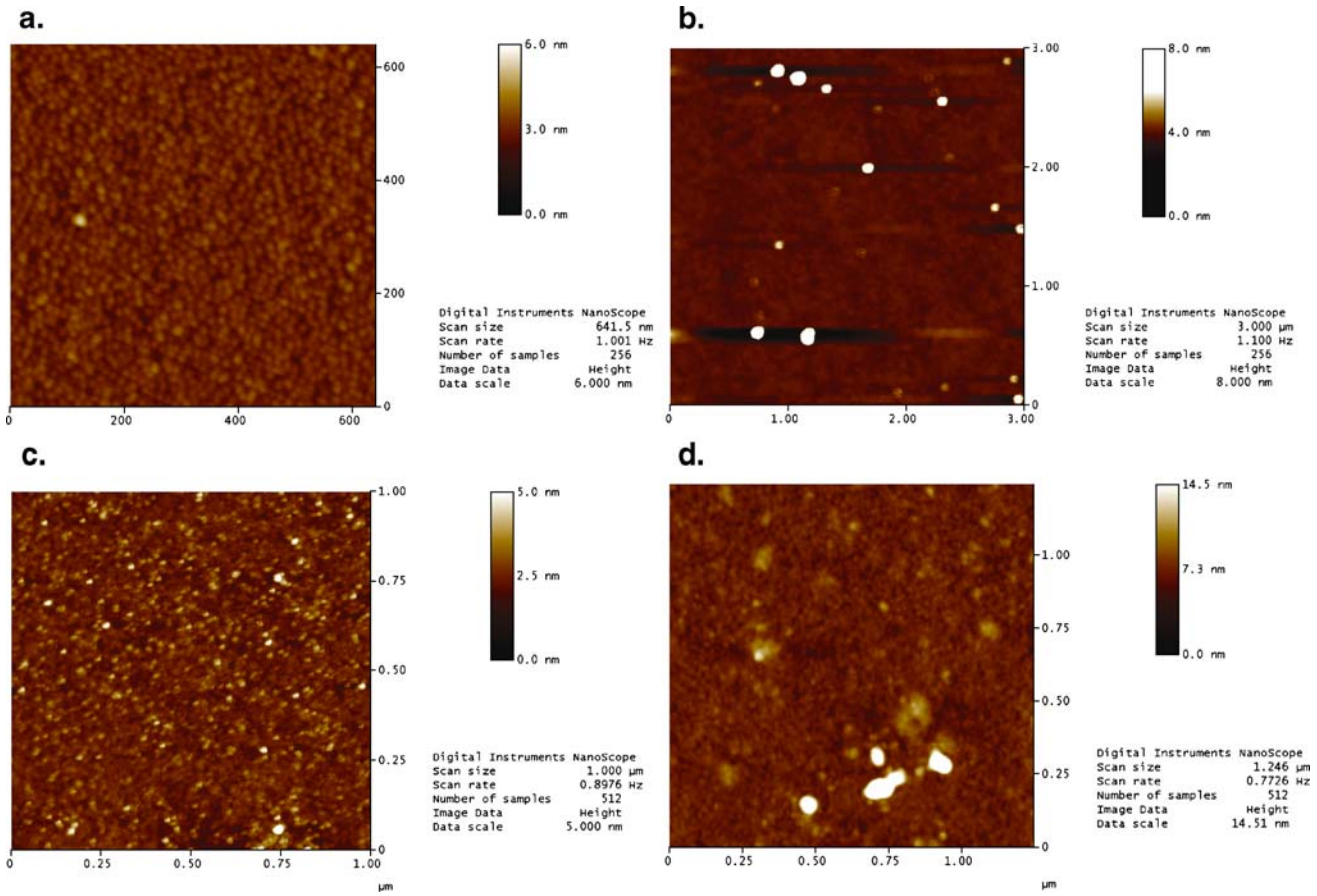

Fig. 5. AFM images of free NC-11 and NC-11/oligonucleotide complexes. The heights of the AFM images are represented by a *graded black-white scale*. (**a**) two-dimensional view of NC-11, (**b**) 2-d view of NC-11/oligonucleotide complex, (**c**) 2-d view of serum only, (**d**) 2-d view of NC-11/oligomer complex in serum. *White color* indicates a height above the silicone wafer. The *x* and *y* dimensions are scaled as shown.

Nondenaturing Polyacrylamide Gel Electrophoresis

Electrophoretic mobilities of DPLs were investigated on 10% polyacrylamide gels using TBE buffer (2.5 mM Na_2EDTA, 80 mM boric acid, 90 mM Tris, pH 8.3) to which was added 0.19 M glycine. Samples were loaded onto gels in a buffer composed of 15% glycerol, 0.025% bromophenol blue and 0.1 mM EDTA and electrophoresed in a reverse electrode at 4°C, 60 V for 100 min. After separation, the gel was placed in 0.25 M bicarbonate buffer for about 5 min at room temperature. It was then transferred to a fresh solution of bicarbonate buffer (containing 0.5 M glutaraldehyde) and incubated at 4°C for 1 h. After fixation, the gels were stained with Coomassie brilliant blue stain. Destaining was carried out in 10% methanol / 10% acetic acid solution (21).

Agarose Gel Electrophoresis of the Complexes of DPLs and Oligonucleotide

Complex formation of DPLs and oligonucleotides was examined by an agarose gel stained with ethidium bromide at the various charge ratios of DPLs to oligonucleotides. The complexes were prepared in TBE buffer (2.5 mM Na_2EDTA, 80 mM boric acid, 90 mM Tris, pH 8.3) at pH 8.3, then loaded with bromophenol blue in glycerol into 1% agarose gel in TBE (45 mM Tris-Borate and 1 mM EDTA, pH 8.0) buffer and electrophoresed at room temperature, 100 V for 15 min. The gel was stained with ethidium bromide (0.5 µg/ml).

Preparation of Oregon Green 488 Conjugated NC-12

Appropriate amount of Oregon green 488 carboxylic acid succinimidyl ester (Molecular Probes) in DMSO (1 mg/ml) were added to the DPL generation 6 (NC-12) in 1 ml of 50 mM sodium borate buffer (pH 8.3), after which stirring continued 4 hr at room temperature. The crude reaction solution was evaporated in a Speed-Vac. The dried pellet was dissolved in a minimum volume of aqueous TFA (0.1%, v/v). Fractions recoved from the Sephadex G25 were analyzed by TLC on a non-fluorescent silica plate using 100% MeOH as the eluent. Under long wavelength UV light, the tagged NC-12 were remained almost immobile at the origin, while unconjugated Oregon green 488 migrated fairly close to the solvent front ($R_f = 0.8$).

Cytotoxicity Assay

Cells were incubated with complexes of oligonucleotides (0.25 µM) and DPLs, with oligonucleotide alone (0.25 µM), or with control medium, for 24 h in 10% FBS/DMEM, rinsed twice with phosphate-buffered saline (PBS), incubated for a further 24 h. The surviving fraction was determined by the MTT dye assay; 50 µl of MTT dye solution (0.5 µg/ml) was added to each well and incubation continued for another 30

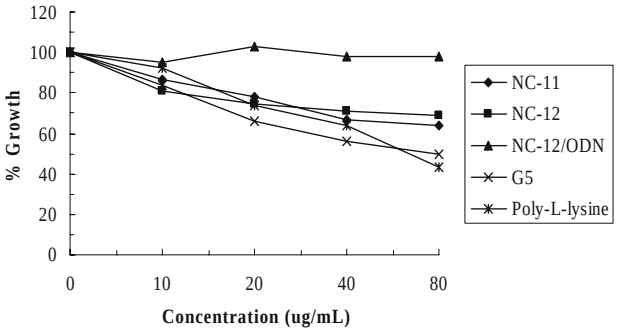

Fig. 6. Acute toxicity assay of DPLs. Generation 5 DPL (NC-11) and generation 6 DPL (NC-12) alone or NC-12/oligonucleotide complex were applied to cells with 10% FBS/DMEM. Cell viability was expressed as percent cells remaining compared to untreated cells or poly-L-lysine treated cells, based on the MTT assay. Data represent the average of three experiments. $p < 0.05$ for NC-12 versus NC-12/ODN complex at 20 μg/ml. ($n = 3$).

min. Absorbance at 540 nm was quantified with an automated microplate reader (MULTISCAN® EX, THERMO).

Antisense Splicing Correction Assay

HeLa cells transfected stably with a reporter gene construct were plated in six-well trays at a density of 3×10^5 cells per well in 3 ml of 10% FBS/DMEM and antibiotics. Cells were maintained for 24 h at 37°C in a humidified incubator (5% CO_2 / 95% air). A 100 ul of aliquot of oligonucleotide at a given concentration in Opti-MEM was mixed with 100 μl of Opti-MEM containing various concentrations of DPLs. After being briefly mixed, the preparation was left undisturbed at room temperature for 5 min, followed by dilution to 1 ml with Opti-MEM before being layered on the cells. The cells were incubated for 6 h and subsequently the medium was replaced with 10% FBS/DMEM. After further 18 h, the cells were rinsed with PBS and lysed in 100 μl of lysis buffer (200 mm Tris-HCl, pH 7.8, 2 mM EDTA, 0.05% Triton X-100) on ice for 15 min. Following centrifugation (1,300 rpm, 2 min), 5 μl of supernatant cell extract was mixed with 100 μl of luciferase substrate (1 mM D-luciferin). The light emission was normalized to the protein concentration of each sample, determined according to the bicinchonic acid assay.

Confocal Microscopy

Subcellular distribution of fluorescent oligonucleotide and DPL (NC-12) in HeLa cells were conducted in a six-well plate containing glass coverslips at a cell density of 3×10^4 cells/well. After transfection with Oregon green 488 labeled DPL/TAMRA-ODN complexes for 5 h, cells were washed twice with PBS, mounted onto glass microscope slide, and processed for laser confocal scanning microscopy (TCS NT, Leica, Germany) to provide cellular location of DPL and oligonucleotide.

RESULTS

DPL Characterization

DPLs were synthesized by using the epsilon-peptide template (a peptide consisting of lysine residues) as an initiator core. DPLs of the second to sixth generations were obtained by coupling Boc-L-Lys(Boc)-OH·DCHA repeatedly after deprotection with TFA (Fig. 1a). The size and complexity of DPL grow rapidly as the number of generation increases (Table I). The predicted number of surface amines increases from 32 for NC-4 (generation 2) to 512 for NC-12 (generation 6), doubling the number of surface amine groups on additional generation. Molecular weight of DPLs was confirmed by MALDI TOF-MS. The schematic structure of DPL generation 6 (NC-12) is shown in Fig. 1b.

Physical Properties of the Prepared DPLs

Physical properties of DPLs were investigated by polyacrylamide gel electrophoresis (PAGE) and capillary zone electrophoresis (CZE). In 10% PAGE under non-denaturing condition, DPLs showed a clear single band and the migration was size and/or charge dependant (Fig. 2a). DPLs were also successfully separated by CZE at acidic pH using uncoated fused-silica capillary. Acidic phosphate buffer was chosen as a running buffer (200 mM phosphate:acetonitrile, 2:1 volume ratio, pH 1.5) to avoid interaction between the silanols on the uncoated capillary wall and the DPL. The electrophoretic mobilities of DPLs in 10% PAGE and CZE was very consistent with the migration order NC-9 > NC-7 > NC-10 > NC-8 > NC-11 > NC-12, suggesting that the migration order of the DPLs was in a good agreement with the number of surface amino groups and their generations (Fig. 2b) (16).

Complex Formation of Oligonucleotide by DPLs

Agarose gel electrophoresis was performed to evaluate the size and/or charge characteristics of DPLs in the formation of complexes with oligonucleotide (Fig. 3). The positively charged primary amino groups on surface of DPLs formed an ionic complex with anionic oligonucleotide. The complex of DPL/oligonucleotide was not detectable in loading well, but the bands of free oligonucleotide disappeared on gel as the N/P ratio (amino groups : phosphate groups) increases, suggesting that DPLs form complexes with

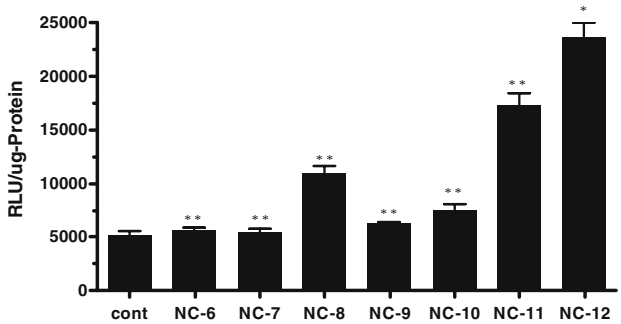

Fig. 7. Comparison of luciferase activity of various generations of DPLs with PAMAM G5 and poly(L-lysine) at optimized concentration of delivery agents. HeLa cell stably transfected with pLuc/705 were treated with optimized concentration (μg/ml) of DPL at fixed concentration (0.15 μM/ml) of a 2′-O-methyl phosphorothioate oligonucleotide. Ordinate: RLU/μg of protein. Control (-) followed by a series of DPLs complexed with oligonucleotide. PL: poly(L-lysine) (20 μg/ml), G5: PAMAM dendrimer generation 5 (20 μg/ml). *Vertical bars* indicate means and standard errors ($n > 3$). *$p < 0.05$ and **$p < 0.01$ versus untreated control at each DPL.

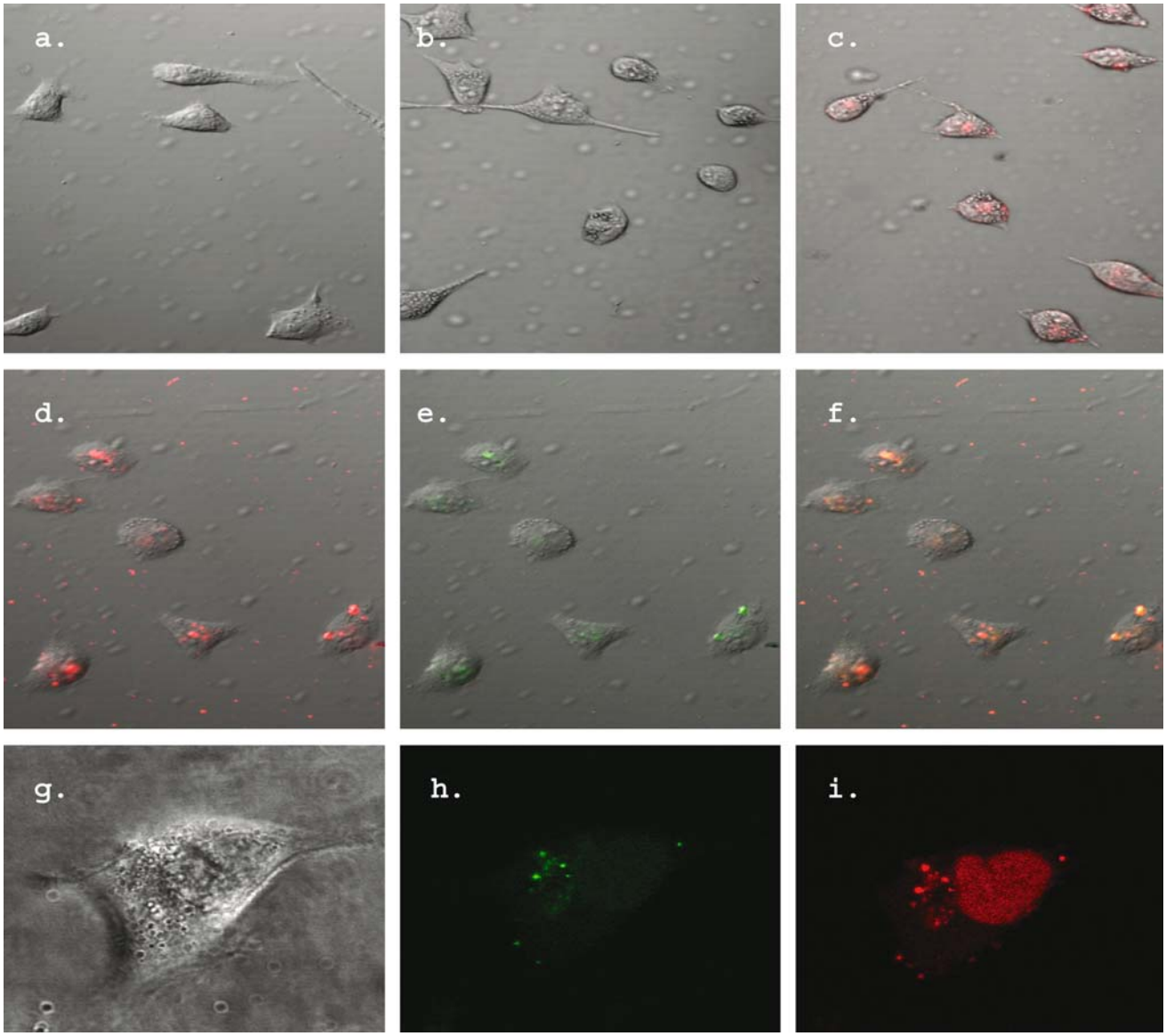

Fig. 8. Confocal microscope images of live cells treated with fluorescent 2′-O-methyl phosphorothioate oligonucleotide. HeLa-Luc cells were treated for 5 h in the presence of 3′-end TAMRA-labelled phosphorothioate oligonucleotide/ORG-NC-12 complex, mounted onto glass microscope slide, and processed for confocal microscopy. (**a**) untreated cells; (**b**) TAMRA-oligonucleotide alone; (**c**) TAMRA-oligonucleotide transfected using Lipofectin (4 μg/ml); (**d–f**) TAMRA-oligonucleotide (0.15 μM)−NC12-Org (20 μg/ml): (**d**) TAMRA-oligonucleotide through *red* channel; (**e**) NC12-Org through *green* channel; (**f**) superimposition of d and e. (**g–i**) subcellular distribution of TAMRA-oligonucleotide-NC12-Org; (**g**) transmission image of the cell; (**h**) vertical section image of NC12-Org through *green* channel; (**i**) vertical section image of TAMRA-oligonucleotide through red channel.

oligonucleotide. The reduction of band intensity of free oligonucleotide was dependent on both N/P ratios and the generation of DPLs with faster decreases for NC-12 compared with lower generation DPLs. Binding properties of DPLs with oligonucleotide were further examined by fluorescent dye exclusion assay, using SYBR Green I (Fig. 4). Rapid reduction in fluorescence intensity was observed in DPLs bound to oligonucleotide because the condensation of oligonucleotide causes the reduction in fluorescence intensity by excluding SYBR Green I from the altered helix structure (8,22). A high generation DPL of NC-11 showed faster reduction in the relative fluorescence intensity than the low generation of NC-4. Interestingly, PAMAM dendrimer generation 5, which has the same number of surface amino groups with NC-10, showed faster condensation to oligonucleotide than a DPL generation 5, NC-11.

Atomic Force Microscopy (AFM)

Topographic images, which were carried out to characterize the morphology of the complexes, are shown in Fig. 5. The morphology of heterogeneous NC-11/oligonucleotide complexes (Fig. 5b) was clearly distinguishable from a homogeneous spherical shape of NC-11 itself (Fig. 5a). The average size of NC-11 and NC-11/oligonucleotide complex were 12.2 and 73 nm, respectively. Interestingly, AMF images

taken with oligonucleotide/NC-11 in the presence of FBS did not show dramatic change in size of the complex (Fig. 5d).

Cytotoxicity of DPLs

The toxic effects of DPL generations and oligonucleotide/DPL complexes on cells were assessed by a MTT dye assay. Figure 6 shows percent cell survival versus concentration for NC-11, NC-12 or NC-12/oligonucleotide complex. Both NC-11 and NC-12 showed a similar decrease in the toxicity after treatment of cells in 10% serum containing medium, while a little bit higher toxicity was observed for poly L-lysine and PAMAM G5 dendrimer. Complexation with oligonucleotides tended to reduce the toxicity of the NC-12.

Comparison of Luciferase Activity at Optimized Concentration

The ability of DPLs to deliver oligonucleotides in pharmacologically active form was examined by using a splicing correction assay that utilizes an antisense oligonucleotide to correct splicing of a mutated intron (23,24). In this assay, only oligonucleotide reaching in nuclei of viable cells permits correct splicing, resulting in luciferase activity. HeLa-Luc 705 cells were treated with various concentrations of DPLs at a fixed concentration (0.15 μM) of 2′-O-Me phosphorothioate oligonucleotide complementary to the β-globin splice site junction. Figure 7 shows the comparison of luciferase activity of various generations of DPLs complexed with oligonucleotides at an optimized concentration of delivery agents. High generation DPLs such as NC-8, NC-11 and NC-12 complexed with oligonucleotide were quite effective with progressive dose–response relationship with respect to the concentration of the DPL, while low generation DPLs complexed with oligonucleotide showed low activities (Fig. 7). NC-11 and NC-12 were moderately active and comparable to PAMAM G5 dendrimer and linear poly(L-lysine). NC-8, a generation 5 DPL with five lysine residues in a core template, had less Luciferase activity than NC-11 or NC-12, but clearly showed a better delivery efficiency than other lower generation DPLs, suggesting that the size and surface amine charge of DPL may play important role for the efficient delivery of antisense oligonucleotide. A generation 4 DPL, NC-10, which has similar number of surface amines with PAMAM generation 5, was not as effective as PAMAM generation 5 dendrimer.

Confocal Microscopy

The intracellular distribution of oligonucleotide and NC-12 in live cells was visualized by laser confocal scanning fluorescence microscopy. Cells were incubated with 3′-TAMRA-oligonucleotide/ORG-NC-12 complexes for 5 h and processed for confocal microscopy. Cells treated with 3′-TAMRA-oligonucleotide/ORG-NC-12 complexes are seen to have a moderate degree of cellular distribution and a significant nuclear fluorescence, while free oligonucleotide shows only a slight degree of cell distribution and no evidence for nuclear accumulation (Fig. 8). Vertical section analyses indicate that most DPLs are not accumulating inside the nucleus, but stay inside the vesicles in the cytoplasm (Fig. 8h).

DISCUSSION

A series of DPLs with various generations and different number of surface amines were prepared to evaluate the potential use as delivery agents for antisense oligonucleotides. The DPLs showed well-defined structural characteristics on gel and capillary electrophoresis with size and charge dependent migration. High generation DPLs which have the increased charge density and molecular size showed better capability to form a compact complex with oligonucleotide.

A pharmacological effectiveness of an antisense oligonucleotide was evaluated by using a rapid and sensitive luciferase reporter assay system that modifies splicing of a β-globin intron inserted into a Luciferase reporter gene. Since splicing occurs only within the nucleus of a living cell, our assay provides a convincing proof that DPL can deliver oligonucleotide into the target compartment of the cells. High-generation DPLs with hyperbranched architecture were better suited for the oligonucleotide delivery, suggesting that the branch structure inside DPL may play important role for the effective delivery. However, heat-induced partial degradation of high generation DPLs, to increase the flexibility of DPL and therefore to improve the transfection efficiency of oligonucleotide, was not effective since heat treated DPL did not changed the Luciferase activity (data not shown) (29). The nuclear delivery of oligonucleotide was further confirmed by the visualization of fluorescent oligonucleotide in the nucleus by confocal microscopy. Our study suggests that the increased charge density and molecular size of high generation DPLs has better capability to form a compact complex with oligonucleotide and are moderately effective in the delivery of oligonucleotide into cells.

In AFM images, NC-11/oligonucleotide complexes have average size distribution at 73 nm with heterogeneous aggregation adducts. Similar size distribution was observed with NC-11/plasmid DNA complexes (16). The observed size of oligonucleotide/NC-11 complexes can be valuable for *in vivo* application if they act as delivery agents in the presence of the serum proteins (14). It is not clear why the size of the complex in AFM images was not increased by the interaction with serum components. AFM images collected in a tapping mode may not be suitable for the detection of nonspecific binding of serum proteins to the complex. Further study for the understanding of DPL mediated oligonucleotide delivery in the serum environments is in process.

The mechanism of DPL mediated oligonucleotide delivery is unclear at this point. It has been suggested for cationic lipid complexes that internalization through endocytosis is followed oligonucleotide release from endosome to the cytoplasm, and then rapid migration of the released oligonucleotide to the nucleus. The same type of mechanisms may apply to DPL-oligonucleotide complexes. A recent report suggests that binding and uptake of dendrimer-DNA complexes depend on membrane cholesterol and raft integrity (17). Ohsaki *et al.* reported *in vitro* gene transfection using dendritic poly(L-lysine)s which is similar to the molecular structure of our DPLs. Efficient gene transfection ability into the cultivated cell lines such as CHO, HeLa, HuH-7 and COS-7 was confirmed, even in the presence of 50% serum, without significant cytotoxicity (8).

The strategy for future investigation will be to modify the surface amines of high generation DPLs with small hydrophobic molecule to enhance the delivery properties (12,25–29). Modification of the size and charge of the cationic surface amines may confer more promising delivery properties of DPLs.

ACKNOWLEDGEMENTS

This work was supported by the Korea Research Foundation Grant funded by the Korean Government (MOEHRD): (Grant number: E00037). Tran Huu Dung was partially supported by the second stage of BK21 from the Ministry of Education & Human Resources Development, Korea.

REFERENCES

1. C. F. Bennett. Antisense oligonucleotides: is the glass half full or half empty? *Biochem. Pharmacol.* **55**:9–19 (1998).
2. C. A. Stein and Y. C. Cheng. Antisense oligonucleotides as therapeutic agents—is the bullet really magical? *Science* **261**: 1004–1012 (1993).
3. S. T. Crooke. Molecular mechanisms of action of antisense drugs. *Biochim. Biophys. Acta* **1489**:31–44 (1999).
4. O. Zephati and F. C. Szoka Jr. Mechanism of oligonucleotide release from cationic liposomes. *Proc. Natl. Acad. Sci. USA* **93**(21):11493–11498 (1996).
5. A. Akinc, M. Thomas, A. M. Klibanov, and R. Langer. Exploring polyethylenimine-mediated DNA transfection and the proton sponge hypothesis. *J. Gene Med.* **7**:657–663 (2005).
6. E. Wagner, M. Cotten, R. Foisner, and M. L. Birnstiel. Transferrin-polycation-DNA complexes: the effect of polycations on the structure of the complex and DNA delivery to cells. *Proc. Natl. Acad. Sci. USA* **15**:4255–4259 (1991).
7. J. P. Leonetti, G. Degols, and B. Lebleu. Biological activity of oligonucleotide-poly(L-lysine) conjugates: mechanism of cell uptake. *Bioconjug. Chem.* **1**(2):149–153 (1990).
8. M. Ohsaki, T. Okuda, A. Wada, T. Hirayama, T. Niidome, and H. Aoyagi. *In vitro* gene transfection using dendritic poly(L-lysine). *Bioconjug. Chem.* **13**(3):510–517 (2002).
9. P. L. Felgner, Y. J. Tsai, L. Sukhu, C. J. Wheeler, M. Manthorpe, J. Marshall, and S. H. Cheng. Improved cationic lipid formulations for *in vivo* gene therapy. *Ann. N.Y. Acad. Sci.* **772**:126–139 (1995).
10. R. DeLong, K. Stephenson, T. Loftus, S. K. Alahari, M. H. Fisher, and R. L. Juliano. Characterization of complexes of oligonucleotides with polyamidoamine starburst dendrimers and effects on intracellular delivery. *J. Pharm. Sci.* **86**:762–764 (1997).
11. H. Yoo, P. Sazani, and R. L. Juliano. PAMAM dendrimers as delivery agents for antisense oligonucleotides. *Pharm. Res.* **16**:1799–1804 (1999).
12. C. C. Lee, J. A. MacKay, J. M. Frechet, and F. C. Szoka. Designing dendrimers for biological applications. *Nat. Biotechnol.* **23**(12):1517–1526 (2005).
13. R. L. Juliano, S. Alahari, H. Yoo, R. Kole, and M. Cho. Antisense pharmacodynamics: critical issues in the transport and delivery of antisense oligonucleotides. *Pharm. Res.* **16**:494–502 (1999).
14. R. L. Juliano and H. Yoo. Aspects of the transport and delivery of antisense oligonucleotides. *Curr. Opin. Mol. Ther.* **2**:297–303 (2000).
15. A. M. Gewirtz, D. L. Sokol, and M. Z. Ratajczak. Nucleic acid therapeutics: state of the art future prospects. *Blood* **92**:712–736 (1998).
16. K. D. Eom, J. S. Kim, S. M. Park, M. S. Kim, R. N. Yu, H. M. Jung, S. G. Kim, and H. Yoo. A facile synthesis and physical properties of nano-sized dendritic α,ε-poly(L-lysine)s for the delivery of nucleic Acids. *J. Nanosci. Nanotechnol.* **6**:3532–3538 (2006).
17. M. Manunta, P. H. Tan, P. Sagoo, K. Kashefi, and A. J. George. Gene delivery by dendrimers operates via a cholesterol dependent pathway. *Nucleic Acids Res.* **32**(9):2730–2739 (2004).
18. T. Okuda, S. Kidoaki, M. Ohsaki, Y. Koyama, K. Yoshikawa, T. Niidome, and H. Aoyagi. Time-dependent complex formation of dendritic poly(L-lysine) with plasmid DNA and correlation with *in vitro* transfection efficiencies. *Org. Biomol. Chem.* **1**(8):1270–1273 (2003).
19. K. D. Eom, J. L. Yang, and J. P. Tam. *Proceeding of the Eighteenth American Peptide Symposium*. 924–925 (2003).
20. D. R. Baker. *Capillary Electrophoresis*, 1st ed. Wiley: A Wiley-Interscience Publication, 1995.
21. A. Sharma, D. K. Mohanty, A. Desai, and R. Ali. A simple polyacrylamide gel electrophoresis procedure for separation of polyamidoamine dendrimers. *Electrophoresis.* **24**:2733–2739 (2003).
22. A. L. Parker, D. Oupicky, P. R. Dash, and L. W. Seymour. Methodologies for monitoring nanoparticle formation by self-assembly of DNA with poly(L-lysine). *Anal Biochem.* **1**:75–80 (2002).
23. H. Sierakowska, M. J. Sambade, S. Agrawal, and R. Kole. Repair of thalassemic human beta-globin mRNA in mammalian cells by antisense oligonucleotides. *Proc. Natl. Acad. Sci. USA* **93**:12840–12844 (1996).
24. S. H. Kang, M. J. Cho, and R. Kole. Up-regulation of the luciferase gene expression with antisense oligonucleotides: implications and applications in functional assay development. *Biochemistry* **37**:6235–6239 (1998).
25. H. Kang, R. DeLong, M. H. Fisher, and R. L. Juliano. Tat-conjugated PAMAM dendrimers as delivery agents for antisense and siRNA oligonucleotides. *Pharm. Res.* **22**(12):2099–2106 (2005).
26. M. Hussain, M. Shchepinov, M. Sohail, I. F. Benter, A. J. Hollins, E. M. Southern, and S. Akhtar. A novel anionic dendrimer for improved cellular delivery of antisense oligonucleotides. *J. Control. Release* **99**(1):139–155 (2004).
27. H. Yoo and R. L. Juliano. Enhanced delivery of antisense oligonucleotides with fluorophore-conjugated PAMAM dendrimers. *Nucleic Acids Res.* **28**(21):4225–4231 (2000).
28. T. I. Kim, H. J. Seo, J. S. Choi, H. S. Jang, J. U. Baek, K. Kim, and J. S. Park. PAMAM-PEG-PAMAM: novel triblock copolymer as a biocompatible and efficient gene delivery carrier. *Biomacromolecules* **5**(6):2487–2492 (2004).
29. M. X. Tang, C. T. Redemann, and F. C. Jr. Szoka. *In vitro* gene delivery by degraded polyamidoamine dendrimers. *Bioconjug. Chem.* **7**(6):703–714 (1996).